

# Fluctuation induced hopping and spin polaron transport

L. G. L. Wegener and P. B. Littlewood  
*TCM, Cavendish Laboratory, Cambridge University,  
 Madingley Road, Cambridge, CB3 0HE, United Kingdom*  
 (Dated: February 1, 2008)

We study the motion of free magnetic polarons in a paramagnetic background of fluctuating local moments. The polaron can tunnel only to nearby regions of local moments when these fluctuate into alignment. We propose this fluctuation induced hopping as a new transport mechanism for the spin polaron. We calculate the diffusion constant for fluctuation induced hopping from the rate at which local moments fluctuate into alignment. The electrical resistivity is then obtained via the Einstein relation. We suggest that the proposed transport mechanism is relevant in the high temperature phase of the Mn pyrochlore colossal magneto resistance compounds and  $\text{EuB}_6$ .

PACS numbers: 72.20.Ee, 72.80.Ga

Keywords: Spin polaron, spin polaron transport, fluctuation induced hopping

Recently Free Magnetic Polarons (FMP) have received renewed attention. They were proposed to explain the Colossal Magnetoresistance (CMR) in the Manganese Pyrochlore compounds<sup>1,2,3,4,5,6</sup> and they have been studied in the context of the double exchange model and the Manganese Perovskite CMR compounds<sup>7,8,9</sup>. Moreover, Raman scattering data has suggested<sup>10,11</sup> that they exist in  $\text{EuB}_6$ . Previous theoretical studies have focussed on the static properties of the FMP. Here we focus on the dynamic aspect, propose a new transport mechanism for a FMP and calculate the resulting resistivity.

A magnetic polaron is a composite object consisting of a localised charge carrier and the alignment it induces in a background of local moments. Localisation can occur for two different reasons: the carrier can be trapped by an impurity atom and then induce a magnetisation in the region where it is localised. The resulting particle is called a “Bound Magnetic Polaron” (BMP). It is well documented experimentally, for example in dilute magnetic semiconductors like  $\text{Cd}_{1-x}\text{Mn}_x\text{Se}$ <sup>12</sup>, and in rare earth chalcogenides<sup>13</sup>. It has been studied in depth theoretically<sup>14</sup>. A BMP is not free to roam through the sample since it is bound to its impurity. Only activated transport is possible: when the BMP is “ionised” the carrier is free to move until it is trapped by the next impurity.

However, for large enough coupling to the local moments the carrier can self-trap without the need for an impurity<sup>15,16,17</sup>, forming a Free Magnetic Polaron (FMP). Due to the coupling the carrier acts as a magnetic field on the local moments. The strength of this field varies in space as the probability density of the carrier: the more localised the carrier the stronger the field and the larger the energy gain resulting from aligning the local moments. The region of aligned moments therefore acts as a potential well that localises the electron and a FMP is formed. The balance between the gain in magnetic energy from induced alignment and the loss in kinetic energy because of localisation determines the polaron size. The existence of an FMP has not been confirmed experimentally, but it has been suggested in the

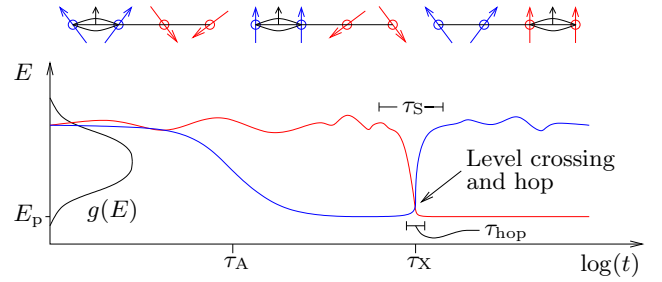


FIG. 1: **Time evolution of electron state.** Black curved lines and arrows in the upper part represent the electron density and spin. A carrier is put on the “blue” level. A hop occurs when the “red” and “blue” levels cross. The density of states  $g(E)$  is shown on the LHS of the lower part.

Mn-pyrochlores<sup>4,5,6</sup> and in  $\text{EuB}_6$  as well<sup>10</sup>.

The mechanism of transport by FMP is in doubt. The conventional view is that transport is necessarily activated, as for a BMP. Here we present an alternative viewpoint: we propose that, unlike the BMP, the FMP can move between nearby sites without thermal assistance. We consider a fluctuating, paramagnetic background of local moments. A neighbouring region of local moments can fluctuate into the same alignment as the polaronic moments. At that moment, the carrier can tunnel to the newly aligned region without needing to overcome an energy barrier. The tunneling process is fast compared to the spin fluctuations. After the tunneling process the carrier and the alignment have moved so that the complete FMP has hopped to the new location. The entire time evolution of the polaron formation and hopping process is illustrated in Figure 1. We call this transport mechanism “Fluctuation Induced Hopping” (FIH). It does not involve an activated process. We calculate the resistivity FIH gives rise to.

In the next section we present a model Hamiltonian that provides the frame of reference for our work. We describe the static properties of the FMP and the band states in Sec. II, postponing a justification until Appendices A and B. In Sec. III we calculate the electrical

resistivity for polaron hopping. We determine the rate at which nearby regions of local moments accidentally align themselves due to fluctuations. Since the FMP tunnels to these regions, this rate determines the diffusion constant and hence the electrical resistivity.

## I. MODEL HAMILTONIAN

We consider a low density electron gas that is coupled ferromagnetically to a background of local moments. The local moments are themselves coupled ferromagnetically. The following Hamiltonian describes this system<sup>1,2</sup>:

$$H = t \sum_{\langle i,j \rangle \sigma} c_{i\sigma}^\dagger c_{j\sigma} - J' \sum_i \vec{\sigma}_i \cdot \vec{S}_i - J \sum_{\langle i,j \rangle} \vec{S}_i \cdot \vec{S}_j. \quad (1)$$

Here  $i$  denotes the lattice site,  $c_{i\sigma}^\dagger$  creates a conduction electron,  $\vec{S}_i$  is the local moment on site  $i$  and  $\vec{\sigma}_i$  is the conduction electron's spin.  $\langle i,j \rangle$  denotes a summation over nearest neighbours. The first term of the Hamiltonian in Eqn. 1 is the kinetic energy of the carriers, the second term couples the carriers to the local moments on which they reside. The third term couples the local moments ferromagnetically. This term can be due to, for example, superexchange. We have an  $s$ - $d$  Hamiltonian with an additional Heisenberg term. We consider the strong coupling regime in which

$$J' \gtrsim t \sim 10J \sim 0.1 \text{ eV}. \quad (2)$$

In our calculations we use the values  $J' = 5t$  and  $J = 0.01\text{eV}$  which are in agreement with experimental values in the relevant materials<sup>1,10</sup>. It should be noted that the magnetic transition is not driven by the  $s$ - $d$  part of the Hamiltonian, but only by the superexchange because of the low carrier density.

## II. POLARON AND BAND STATE

Here we present the wave function we use to study the transport properties of the FMP. Our variational calculation in Appendix A shows that the FMP is small in the strong coupling regime: the carrier occupies approximately two lattice sites (see Figure 3). We therefore use the following wave function to describe the polaron:

$$|P\rangle = \frac{1}{\sqrt{2}}(c_0^\dagger + c_1^\dagger) |0\rangle \otimes |\uparrow\rangle_{\vec{m}} \otimes |\vec{m}\rangle, \quad (3)$$

where  $\vec{S}_i$  are the polaronic local moments and  $\vec{m} = \vec{S}_0 + \vec{S}_1$  is the magnetisation of the FMP. It describes a carrier localised on two lattice sites, with its spin quantised and pointing “up” along the direction of  $\vec{m}$  to minimise the  $s$ - $d$  energy. The  $s$ - $d$  term in the Hamiltonian therefore reduces to  $-J'\sigma m$ , which is lower for more aligned local moments. This means that the carrier introduces an additional coupling between the polaronic

moments. The value of the effective coupling constant can be obtained by expanding the expression for  $m$  up to first order in  $\vec{S}_0 \cdot \vec{S}_1 - S^2$  for nearly aligned polaronic moments. We obtain

$$J_{\text{eff}} = \frac{J'}{\sqrt{1 + 8S(2S + 1)}} + 2J. \quad (4)$$

Since  $T \ll J'$  the moments are nearly aligned, so the polaron energy is

$$E_p = -|t| - (J' \sqrt{2S(2S + 1)}/2 + 2JS^2). \quad (5)$$

In addition to the polaron state with its induced magnetisation there are many more possible states for the carrier in which it does not align any local moments. These are states in the narrowed band described in Ref. 18. Since the background fluctuates, these “band states” persist at a given location only for a time comparable to the timescale of these fluctuations, which we denote  $\tau_S$ . Nevertheless, the FMP would be unstable if a significant number of lower energy band states existed, since the carrier could then tunnel to them and gain energy.

To check whether the FMP is stable we need to estimate the position of the band edge. If the polaron level lies below the band edge, band states with a lower energy are exceedingly rare, and can be neglected. If on the other hand the band edge lies below the energy of the FMP, the latter is unstable. We determine the position of the band edge as the lowest energy of a typical band state. We use a variational approach to calculate this energy (details are given in Appendix B). The size of the band state is determined by the balance of the kinetic energy cost of localisation and the gain from the  $s$ - $d$  term. The latter is very small: the carrier aligns its spin with the total magnetisation of the region it is localised in. This magnetisation is due to statistical fluctuations in the paramagnetic regime, and consequently very small. We therefore expect the kinetic term to dominate and the band state to be very large. This is confirmed by our calculation. We show that typical band states are extended over a region of roughly  $10^6$  lattice sites. Their total energy is very close to  $-6t$  (See Equation (B3)). Therefore the polaron level lies below the band edge in the regime we consider ( $J' \gtrsim t$ ), and the FMP is stable. This concludes our discussion of the static properties of the FMP and the band state. In the next section we determine their dynamic properties.

## III. FLUCTUATION INDUCED HOPPING

In this section we consider the FIH mechanism in detail and calculate the hopping rate of the polaron and the resulting electrical resistivity. Let us examine the time evolution of a single carrier that is injected onto a lattice site in an empty system. The local moments in its vicinity cannot respond immediately to the carrier's presence, but react on a timescale  $\tau_A$ . On timescales smaller

than  $\tau_A$ , the background appears static. A completely static background would cause Anderson localisation<sup>18</sup> and trap the carrier in a state in the tail of the band below the mobility edge. Although localised, the carrier has not yet induced any alignment between local moments in its vicinity; it is in one of the band states described above. Only when the moments have aligned themselves is the energy of the state greatly reduced. This means that there is a large energy barrier that prevents the carrier from making thermal hops out of the region of alignment. However, the energy of band states fluctuates because the local moments fluctuate. It can therefore cross the polaron level. At such a crossing the electron can tunnel to this level, since there is no more energy barrier to overcome. We call this tunnelling process Fluctuation Induced Hopping (FIH). After the electron tunnelled, the entire FMP has moved: carrier and alignment have jumped to another site. We summarise the entire time evolution in Fig. 1.

The occurrences of hops are uncorrelated in time and space since the background of local moments is paramagnetic. FIH is therefore a Markoff process and the FMP executes a random walk. In an ensemble of realisations of the polaron and the background, polarons in different realisations follow different paths. The Probability Density Function (PDF) of the polaron, defined as the fraction of realisations in an ensemble that have the FMP at a specified time at a specified location, obeys the diffusion equation.<sup>19</sup> The diffusion constant in this equation characterises the polaron transport in the long time limit.

For a random walk in three dimensions that consists of hops of  $l$  lattice constants, occurring with a frequency  $\omega_l$ , the diffusion constant is:<sup>20</sup>

$$D = \frac{1}{6} \sum_{l=1}^{\infty} (la)^2 \omega_l, \quad (6)$$

where  $a$  is the lattice constant. The resistivity from polaron transport is then obtained from the diffusion constant by means of the Einstein formula:

$$\rho = (ne\mu)^{-1} = \frac{k_B T}{ne^2 D}, \quad (7)$$

where  $\mu$  is the mobility, and  $n$  the number density of polarons.

### A. Rate of level crossings

We calculate the rate at which band state levels cross the polaron level. Such a crossing occurs when the band state energy fluctuates so much that it lies at or below the polaron level. The crossing rate depends on the size of the band state: the energy gap between the FMP and band states depends on their size. In addition to this, we will see that the energy of large band states fluctuates less. First we calculate the crossing rate for small band states.

The energy difference between the polaron and a small band state is only due to the difference in exchange energy since their kinetic energies are identical. The time at which the RMS deviation of the band state energy becomes as large as the energy gap between the two levels therefore determines the crossing rate.

$$\begin{aligned} & \langle (\vec{S}_0 \cdot \vec{S}_1)_{J_{\text{eff}}} - \langle \vec{S}_0 \cdot \vec{S}_1 \rangle_J \rangle^2 = \\ & \langle [\vec{S}_0(\tau_X) \cdot \vec{S}_1(\tau_X) - \vec{S}_0(0) \cdot \vec{S}_1(0)]_J^2 \rangle, \end{aligned} \quad (8)$$

where angular brackets denote ensemble averaging. We neglect the variance of the polaronic exchange energy since it is very small due to the large effective coupling constant of the polaronic moments (See Appendix II). We also neglect the exchange energy of the band state compared to the polaron exchange energy:

$$\begin{aligned} & \langle [\vec{S}_0(\tau_X) \cdot \vec{S}_1(\tau_X)] [\vec{S}_0 \cdot \vec{S}_1]_J \rangle = \\ & \langle [\vec{S}_0 \cdot \vec{S}_1]^2 \rangle_J - \frac{1}{2} \langle \vec{S}_0 \cdot \vec{S}_1 \rangle_{J_{\text{eff}}}^2. \end{aligned} \quad (9)$$

For simplicity we use an interpolation between  $t = 0$  and  $t = \infty$  instead of the exact analytical form of the four-point correlator in Eqn. 9. At time  $t = 0$  the correlator reduces to  $\langle (\vec{S}_0 \cdot \vec{S}_1)^2 \rangle$ . A pair of spins at  $t = 0$  is completely uncorrelated with itself at  $t = \infty$ , so that in this limit the correlator reduces to  $\langle \vec{S}_0 \cdot \vec{S}_1 \rangle^2$ . We can therefore interpolate as follows:

$$\begin{aligned} & \langle [\vec{S}_0(t) \cdot \vec{S}_1(t)] [\vec{S}_0(0) \cdot \vec{S}_1(0)] \rangle = \\ & \langle (\vec{S}_0 \cdot \vec{S}_1)^2 \rangle - f\left(\frac{t}{\tau_S}\right) \left[ \langle (\vec{S}_0 \cdot \vec{S}_1)^2 \rangle - \langle \vec{S}_0 \cdot \vec{S}_1 \rangle^2 \right], \end{aligned} \quad (10)$$

where  $f(x)$  varies smoothly from 0 at  $x = 0$  to 1 at  $x = \infty$ . Moreover, we have written  $f(t/\tau_S)$  since the four-point correlator varies on the same timescale as the fluctuations of the background. This allows us to rewrite Eqn. 9 as:

$$f\left(\frac{t}{\tau_S}\right) = \frac{\frac{1}{2} \langle \vec{S}_0 \cdot \vec{S}_1 \rangle_{J_{\text{eff}}}^2}{\langle (\vec{S}_0 \cdot \vec{S}_1)^2 \rangle_J - \langle \vec{S}_0 \cdot \vec{S}_1 \rangle_J^2}. \quad (11)$$

Since  $f(x)$  is a smooth function varying between 0 and 1 that changes mostly near  $x = 1$ ,  $f(1) \approx 1/2$  and  $f'(1) \approx 1$ . We expand  $f(t/\tau_S)$  up to first order about  $t = \tau_S$ , which yields

$$\frac{\tau_X}{\tau_S} \propto \frac{\langle \vec{S}_0 \cdot \vec{S}_1 \rangle_{J_{\text{eff}}}^2}{\langle (\vec{S}_0 \cdot \vec{S}_1)^2 \rangle_J - \langle \vec{S}_0 \cdot \vec{S}_1 \rangle_J^2}. \quad (12)$$

This means that crossings occur on the time scale of the fluctuations of the Heisenberg magnet weighted by the different alignments of the polaron and the background spins. Since  $k_B T \ll J'$ , the numerator of Eqn. 12 reduces to  $(S(S+1))^2$ .

For  $k_B T \gtrsim \mathcal{O}(J)$  the two terms in the denominator of Eqn. 12 have very similar temperature dependences, so that

$$\tau_X = A \tau_S \frac{(S(S+1))^2}{\langle \vec{S}_0 \cdot \vec{S}_1 \rangle_J^2}, \quad (13)$$

where  $A \sim \mathcal{O}(1)$ . We use the expression given in Ref. 21 in the denominator and  $\tau_S = \hbar\sqrt{\beta/J}$ .<sup>22</sup> to obtain

$$\tau_X = A \frac{\hbar}{J} (\beta J)^{-\frac{3}{2}}. \quad (14)$$

$\tau_X$  increases with temperature. With increasing temperature level crossings become more rare. The decrease in the timescale of the spin fluctuations is more than offset by the increase of the average misalignment of the local moments.

For  $k_B T \gg J$  the temperature dependences differ:  $\langle (\vec{S}_0 \cdot \vec{S}_1)^2 \rangle$  tends to  $S^2/3$  since the spins are completely uncorrelated, whereas  $\langle \vec{S}_0 \cdot \vec{S}_1 \rangle_J$  vanishes as  $1/T$ . Moreover the timescale of the fluctuations is different:<sup>23</sup>  $\tau_S = \hbar/\sqrt{S(S+1)J}$ . Hence  $\tau_X$  tends to a constant in this limit:

$$\tau_X = \frac{3\hbar}{J\sqrt{S(S+1)}}. \quad (15)$$

The reason is that the local moments are completely disordered in this regime; an increase in temperature does not cause an increase in disorder. The crossover between the two regimes occurs at a temperature of about  $JS(S+1)/k_B$ .

Equations (14) and (15) constitute the principal result of this section. However, before proceeding to the estimate of the diffusion constant we should check that fluctuations of other band states - in particular those involving rearrangements of many spins - do not change our conditions. We calculate the crossing rate of large band states with the polaron level in the same way as before (see Appendix C for details). For a level crossing with a large band state, many local moments need to fluctuate into alignment simultaneously. This is a very unlikely event, and one expects the crossing rate to be accordingly small. This expectation is borne out by our calculation. In Appendix C we show that level crossings with large band states can be neglected safely.

## B. Diffusion Constant

When a crossing occurs it is possible, but not necessary, for the FMP to hop. The probability,  $\mathcal{P}_l$ , of a hop of length  $l$  at a level crossing depends on the overlap between polaron and band state wave functions and on the rate at which the levels cross. The frequency at which hops of length  $l$  occur,  $\omega_l$ , is then

$$\omega_l \propto l^2 \tau_X^{-1} \mathcal{P}_l, \quad (16)$$

since the number of small band states a distance  $l$  away from the FMP is roughly proportional to  $l^2$ . The tunnelling probability from the polaron state,  $|P\rangle$ , to the band state,  $|B\rangle$  with energies  $E_P$  and  $E_B$  is given by the Landau-Zener formula<sup>24,25</sup>

$$\mathcal{P}_{P \rightarrow B} = 1 - \exp \left[ -\frac{2\pi}{\hbar} \frac{|\langle P|H|B\rangle|^2}{\left| \frac{\partial}{\partial t}(E_P - E_B) \right|} \right], \quad (17)$$

where  $H$  is the Hamiltonian for the particle. Here we have  $\left| \frac{\partial}{\partial t}(E_P - E_B) \right| \sim J'S/\tau_S$ , since the energy difference is due to the initially unaligned local moments in the band state. The time in which this difference between the levels disappears is  $\tau_S$ . The spatial extent of the wave functions of the polaron and the small band state limits the hopping range to one lattice constant. The overlap between neighbouring small polaron states given is by:

$$\langle A|H|B\rangle = \frac{1}{2} \langle 0|(c_0 + c_1)H(c_1^\dagger + c_2^\dagger)|0\rangle = -t - \frac{J'}{2}, \quad (18)$$

where the sites 0 and 1 are nearest neighbours and 1 and 2 are nearest neighbours. Therefore the hopping probability at a level crossing between two neighbouring energy levels is given by:

$$P_{A \rightarrow B} = 1 - \exp \left[ -2\pi \frac{(t + J'\sqrt{2S(2S+1)/2})^2}{JJ'} \sqrt{\frac{\beta J}{S}} \right] \approx 1, \quad (19)$$

since  $1 \ll J'/J$ . This means also that the probability is largely independent of temperature. We will therefore take the hopping probability at a level crossing between two neighbouring levels to be 1. The diffusion constant and resistivity for FIH are therefore

$$\begin{aligned} D &\propto a^2 \frac{J}{\hbar} (\beta J)^{\frac{3}{2}} && \text{for } k_B T \gtrsim J \\ D &\propto \text{const.} && \text{for } k_B T \gg J \\ \rho &\propto \frac{\hbar}{ne^2 a^2} (k_B T/J)^{\frac{5}{2}} && \text{for } k_B T \gtrsim J \\ \rho &\propto \frac{\hbar}{ne^2 a^2} k_B T/J && \text{for } k_B T \gg J \end{aligned} \quad (20)$$

This is our main result. We plot the resistivity versus temperature in Figure 2 interpolating between the high and the extremely high temperature regime. Firstly, the FMP can only hop to neighbouring sites when a favourable statistical fluctuation aligns the local moments. These fluctuations are statistically likely in the sense that they can be estimated from the RMS deviation of the spin fluctuations. Occurrences of alignment far from the polaron do not lead to hopping. Secondly, while small polarons typically hop by this process, large ones cannot. The required spin fluctuation into the correct configuration is statistically very rare. Thirdly, the timescale of the spin fluctuation is slow enough that the FMP hops with probability 1 once the requisite configuration is obtained. Fourthly, the diffusion constant decreases and the resistivity increases as a function of temperature. This reflects the increasing time intervals between the level crossings for higher temperatures and the relation between the resistivity and the diffusion constant.

The resistivity we obtained is “metallic”: it increases with temperature, even though we are not considering a metallic system at all. It is interesting to compare our result to the resistivity of a very dirty metal, where  $k_F \lambda_f \approx 1$ ,  $\lambda_f$  being the mean free path for the carriers.

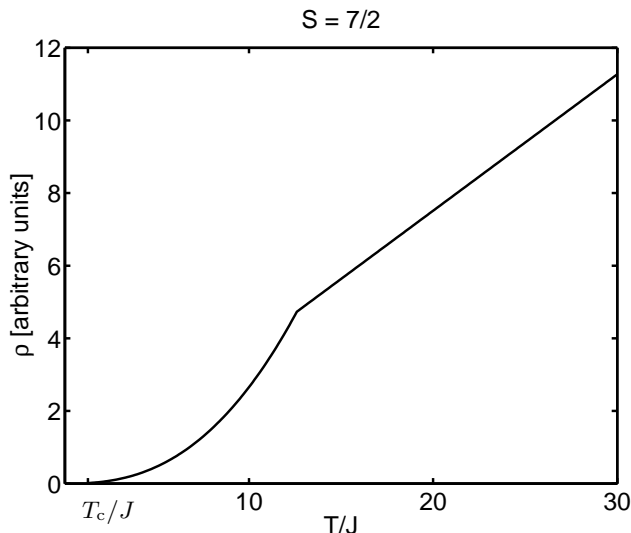


FIG. 2: Temperature dependence of the resistivity.

In such a material the Drude formula for the resistivity yields:

$$\rho = \frac{\hbar}{ne^2\lambda_f^2}. \quad (21)$$

It is clear that despite its temperature dependence the polaron hopping resistivity is far too large to be confused with scattering of metallic carriers. The mean free path in the dirty metal would need to approach one lattice constant for the resistivities to be comparable. At such short mean free paths the metallic picture of delocalised carriers breaks down.

#### IV. CONCLUSIONS

We have proposed a new transport mechanism for FMP in a fluctuating disordered background of local moments. In our theory the FMP hops at the occurrence of a favourable fluctuation. The transport mechanism is therefore not activated, but gives rise to a “metallic” resistivity. Experimentally our theory can be checked by a measurement of the temperature dependent resistivity. Such measurements have been performed in two systems in which the presence of a FMP has been suggested: the Mn-pyrochlores and  $\text{EuB}_6$ .

In the Mn-pyrochlores<sup>6,26,27</sup> the resistivity decreases with increasing temperature above  $T_c$ . This is not in accord with our predictions. There are several reasons for this. There are different types of disorder that affect the resistivity, but were not taken into account in our work. In the In-doped compounds<sup>26</sup>, there is a miscibility gap for dopings of  $0.5 \leq x \leq 1.5$ . In this regime the bulk consists of two types of grains, each of a distinct phase with a different lattice parameter. Transport is dominated by processes associated with the grain boundaries.

Phase separation is suspected to occur in the Sc-doped materials as well. A different type of disorder occurs in Bi-doped compounds: a Bi ion introduces a strong-scattering 6s vacancy on the Tl-sublattice. This could bind the polaron, making its hopping activated. Both the scattering centres and the grain boundaries make the predicted resistivity difficult to observe.

$\text{EuB}_6$  is a much cleaner system, in which magnetic polarons have been observed by spin flip Raman scattering experiments.<sup>10,11</sup> There is good qualitative agreement with experiment in the high temperature paramagnetic regime. The resistivity increases rapidly with temperature up to about 150K and then more slowly; at temperatures above 200K the resistivity increases even more slowly.<sup>28,29</sup> This agrees qualitatively with the crossover we predict. The crossover temperature we predict, 225K is only a little bit too large. The slowdown above 200K is probably due to other scattering mechanisms for the local moments, such as spin-orbit coupling and scattering by carriers. There is no quantitative agreement as no  $T^{5/2}$  law is observed. This is probably due to material specific complications that our theory does not take into account:  $\text{EuB}_6$  exhibits two distinct magnetic transitions between phases with different magnetic anisotropies.<sup>29</sup>

There is good agreement as well with the 2-dimensional Monte Carlo simulation<sup>3</sup>. The simulation and our work agree qualitatively on the static characteristics of the polaron, such as the temperature and  $J'$  dependence of its size and the core magnetisation. We also agree on the temperature window in which the FMP exists. We do not expect more than qualitative agreement given the different parameter regimes that were explored: the simulation uses a much weaker superexchange coupling. The discrepancy between the results for the binding energy in the critical regime can be understood. The simulations show a decrease in magnitude with temperature and we predict an increase. This is due to the breakdown of our high temperature approximation. This also explains why the simulation observes a larger polaron: we neglect the correlations between local moments except those induced by the presence of the carrier, whereas the simulation takes all correlations into account.

The results for the dynamic characteristics of the FMP are different. The simulation shows a diffusion constant that is nearly independent of temperature. This result does not take into account the decrease of the timescale of the fluctuations: the diffusion constant is calculated as the average hopping per unit Monte Carlo time, defined as the number of rediagonalisations. To correct for this we divide the numerical diffusion constant by  $\tau_5$ . This correction increases the discrepancy since the diffusion constant now decreases as a function of temperature. The discrepancy between the corrected Monte Carlo diffusion constant and our result indicates that the simulation looks at a slightly different form of polaron transport. In the simulation the polarons are larger than in our work. Larger polarons can move if a shell of neighbouring local moments aligns themselves. This motion

“through accretion” was not taken into account in our result, which was derived for a small FMP. Our theory and the Monte Carlo simulation do therefore agree qualitatively where agreement is expected.

### Acknowledgments

We would like to thank Professor Khmel'nitskii, Dr. B. D. Simons, Dr. M. Côté, Dr. I. Smolyarenko, M. Calderón, M. L. Povinelli, P. Eastham, and V. Tripathi for fruitful discussions. This work was supported in part by EPSRC and Trinity College Cambridge.

## APPENDIX A: SMALL SPIN POLARONS

We determine the size and energy of the FMP in strong coupling regime by a variational calculation. We choose a trial wave function for the carrier and obtain the electron density at the local moments, which acts as an external field on the moments. The resulting alignment and decrease in energy is calculated using Curie-Weiss theory. The expectation value of the energy of the trial wave function is then minimised with respect to the size of the wave function.

A Gaussian-like function is used for the electronic part of the trial wave function for the FMP; in the notation of Eqn. 1:

$$|P\rangle = \frac{1}{\sqrt{\mathcal{N}}} \sum_{\vec{r}_i} e^{-(r_i/\lambda)^2} c_{\vec{r}_i}^\dagger |0\rangle \otimes |\uparrow\rangle_{\vec{m}} \otimes |\vec{m}\rangle, \quad (\text{A1})$$

where the vectors  $\vec{r}_i$  are the positions of the lattice sites, measured from the centre of the polaron and  $\mathcal{N}$  ensures proper normalisation.  $|\uparrow\rangle_{\vec{m}}$  denotes the electrons spin, which is quantised and pointing “up” along the direction of the average magnetisation induced by the carriers presence.  $|\vec{m}\rangle$  is the state vector of the polaronic local moments. The wings of this wave function take into account that a trapped electron can nearly always make short excursions to a neighbouring non-polaronic local moment. This is possible since it has nearly always a spin component parallel to this moment. These excursions diminish the polaron energy insofar as they reduce the magnetisation of the core through a reduced electron density.

The magnetisation of the background resulting from the presence of the carrier is obtained from Curie-Weiss theory:

$$m(\vec{r}) = \frac{3}{2} B_{\frac{3}{2}} \left[ \beta \left( Jm + \frac{J'}{2} \rho_{\vec{r}_i} \right) \right], \quad (\text{A2})$$

where  $B$  is the Brillouin function and  $\rho_{\vec{r}_i}$  is the electron density at site  $\vec{r}_i$ . Curie-Weiss theory neglects spatial correlations between the local moments that are not due to the effective field of the carrier and the induced magnetisation itself. These spatial correlations are small in

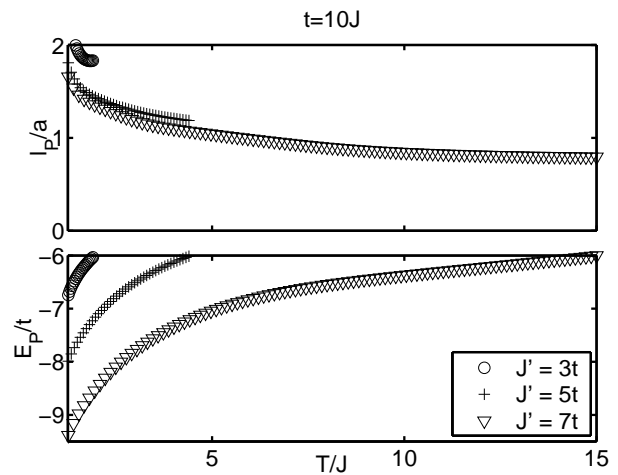


FIG. 3: **Polaron Size vs. Temperature.** The curves stop when the polaron energy reaches the edge of the band (estimated in Sec. B).

a paramagnet, since the coupling constant of the non-polaronic moments is much smaller than the effective field in the core of the FMP ( $J \ll J'$ ). Curie-Weiss theory is therefore accurate in the core of the polaron. In the critical regime non-polaronic correlations become important. Our theory is not valid there.

The expectation value of the energy of the trial wave function is minimised numerically with respect to the size,  $\lambda$ , of the polaron. The results are shown below in Fig. 3. We see that the FMP is small: its size is of the order of a lattice constant over a wide range of temperatures for realistic values of the parameters. The calculated magnetisation is always close to saturation in the core of the polaron, but decreases slightly as a function of temperature. For higher temperatures the FMP shrinks and its energy increases. This is because at constant size the energy gain from the  $s$ - $d$  term decreases as the temperature is raised. To compensate the polaron shrinks, so that the effective field due to the carrier increases, which results in a magnetic energy gain. Hence, at higher temperatures, the point of minimum energy is shifted towards smaller sizes. This also means that a smaller  $s$ - $d$  coupling increases the size. The increase of the polaron energy with temperature can be understood as follows: the kinetic energy is independent of temperature and a decreasing function of size. The magnetic energy curve shifts up as temperature is raised and is an increasing function of size. Therefore, the minimum value of the total energy increases with temperature. These results are in close agreement with Ref. 1 which refers specifically to the pyrochlores.

Our calculation is well-behaved at the ferromagnetic transition, even though this temperature lies outside its range of validity. As  $T_c$  is approached from above, the polaron size tends to a value of approximately  $-9.4t$  at  $T_c$ . Neither the present calculation, nor Ref. 1 takes the

correlations of local moments outside the FMP into account. The predicted size is therefore too small in the critical regime and the energy is overestimated.

## APPENDIX B: BAND STATES

We check whether the FMP we discovered in the previous section is bound by comparing its energy with the position of the band edge. We determine the position of the band edge as the lowest energy of a typical “band states”. The energy of a band state is the difference between the energy of the system with an electron present in that state and the energy of the system in the absence of that electron. Again we use a variational approach with a trial wave function similar to Eqn. A1, with the caveat that local moments are not aligned. Only the kinetic and the  $s$ - $d$  term of the Hamiltonian in Eqn. 1 contribute to the energy, the Heisenberg term is the same regardless of the presence of the carrier in a band state. The kinetic energy of a localised state is determined as before. The magnetic energy is estimated as follows. There is no net magnetisation in the paramagnet, so the  $s$ - $d$  term in the Hamiltonian vanishes on average. In a finite region however, there are statistical fluctuations that make it deviate from this average value, so that there is a non-zero magnetisation in this region,  $\vec{m}_{\text{fluct}} = \sum_i \rho_{\vec{r}_i} \vec{S}_{\vec{r}_i}$ . The carrier’s spin is quantised along the direction of  $\vec{m}_{\text{fluct}}$ , pointing “up”. The average value of the  $s$ - $d$  term in the Hamiltonian is then

$$E_{s-d} = -\frac{J'}{2} \left\langle \sqrt{\sum_{ij} \rho_{\vec{r}_i} \rho_{\vec{r}_j} \vec{S}_{\vec{r}_i} \cdot \vec{S}_{\vec{r}_j}} \right\rangle. \quad (\text{B1})$$

The above sum is split up in one where  $i = j$  and one where  $i \neq j$ . We then take the thermal average of the Taylor expansion of the square root about the  $i = j$  term. The sum that contains term with  $i \neq j$  is at least of order  $\beta J$  since it contains correlations between different local moments. The  $s$ - $d$  energy of the band state is then given by

$$E_{s-d} = -\frac{J'S}{2} \sqrt{\sum_i \rho_{\vec{r}_i}^2} [1 + \mathcal{O}(\beta J)]. \quad (\text{B2})$$

The energy of the band state is minimised numerically with respect to the size. We obtain a size of the order of  $10^6$  local moments that decreases weakly with increasing  $J'$ . We find that the  $s$ - $d$  energy is completely negligible and that the band state is so large that its energy is very close to  $-6|t|$ . We expand the band state energy to second order in  $1/l$  for large  $l$  and obtain:

$$E_{\text{Band}} = -6|t|(1 - \frac{1}{l^2}) - \frac{J'S}{2} \sqrt{\frac{1}{(\sqrt{2}l)^3}}, \quad (\text{B3})$$

where  $l$  is the spatial extent of the band state. The polaron level lies therefore below the band edge and the FMP is well bound.

## APPENDIX C: CROSSING RATE WITH LARGE BAND STATES

We use the same method to calculate the crossing rate for large band states. However, instead of two spins fluctuating into nearly exact alignment many spins need to collectively fluctuate into a more aligned configuration. The time between two crossings is again estimated from the time it takes for the RMS deviation of the band state energy to become as large as the energy difference between the band level and the polaron level:

$$\langle \{E_N[\tau_X(N)] - E_N(0)\}^2 \rangle = (E_P - E_N)^2. \quad (\text{C1})$$

Here  $\tau_X(N)$  is the average time between crossings of the polaron level and a particular band state of  $N$  local moments with energy  $E_N$ . In Appendix B we calculate energy of the band state using a variational Ansatz with an accurate Gaussian trial wave function to show that the FMP is bound. Here, however, we determine the crossing rate and we will see that a simple model is sufficient. We assume that the carrier is localised uniformly without inducing extra alignment. Its spin quantised along the direction of the sum of all the local moments in the band state,  $\vec{m}$ , pointing “up”. The kinetic energy of the band state is approximately  $-6|t|(1 - \pi^2/N^{2/3})$  and its exchange energy vanishes on average. The kinetic energy is constant in time, so it cancels out in the LHS of Eqn. C1, leaving only the RMS deviation of the exchange energy.

Now we use the expression for the 2-site polaron of Eqn. 5 on the RHS of Eqn. C1. The band state  $s$ - $d$  energy can be expressed as  $\sigma m(t)/N^2$  and hence Eqn. C1 becomes:

$$\left[ \left\langle \left\{ \sum_{i,j,k,l}^N [\vec{S}_{\vec{r}_i}(t) \cdot \vec{S}_{\vec{r}_j}(t)] [\vec{S}_{\vec{r}_k}(0) \cdot \vec{S}_{\vec{r}_l}(0)] \right\}^{\frac{1}{2}} \right\rangle \right]_{t=0}^{t=\tau_X(N)} = 2N^2 \left[ \left( 5 - \frac{\pi^2}{N^{2/3}} \right) \frac{|t|}{J'} - \frac{S}{2} \right]^2. \quad (\text{C2})$$

The sum on the LHS of this equation contains  $N^2$  terms of the form  $S^4$  and  $2N$  terms of the form  $S^2 \sum_{i \neq j}^N \vec{S}_{\vec{r}_i} \cdot \vec{S}_{\vec{r}_j}$  where the spin operators are evaluated at equal times. There are also terms where  $i \neq j$  and  $k \neq l$ . The square root is expanded about the term of order  $N$ :

$$\begin{aligned} & \left\{ \sum_{i,j,k,l}^N [\vec{S}_{\vec{r}_i}(t) \cdot \vec{S}_{\vec{r}_j}(t)] [\vec{S}_{\vec{r}_k}(0) \cdot \vec{S}_{\vec{r}_l}(0)] \right\}^{\frac{1}{2}} = \\ & \quad + NS(S+1) + \sum_{i \neq j}^N \vec{S}_{\vec{r}_i} \cdot \vec{S}_{\vec{r}_j} + \\ & \quad + \sum_{i \neq j, k \neq l}^N \frac{[\vec{S}_{\vec{r}_i}(t) \cdot \vec{S}_{\vec{r}_j}(t)] [\vec{S}_{\vec{r}_k}(0) \cdot \vec{S}_{\vec{r}_l}(0)]}{2NS(S+1)} + \dots \end{aligned} \quad (\text{C3})$$

Thermal averaging both sides of this equation results in many two- and four-point spin correlators. We only retain the correlators of lowest (quadratic) order in the

small parameter  $\beta J$ , thereby considering only nearest neighbour interactions. Moreover, the first and second terms on the RHS of Eqn. C3 cancel in Eqn. C2 since they do not depend on time. Hence the condition for a level crossing reduces to

$$\left\langle (\vec{S}_0 \cdot \vec{S}_1)^2 - \{\vec{S}_0[\tau_X(N)] \cdot \vec{S}_1[\tau_X(N)]\}[\vec{S}_0 \cdot \vec{S}_1] \right\rangle = \frac{2S(S+1)N^2}{3} \left[ \left(5 - \frac{\pi^2}{N^{2/3}}\right) \frac{|t|}{J'} - \frac{S}{2} \right]^2. \quad (\text{C4})$$

The four-point correlator is treated as in Eqn. 10 and we introduce the numerical constant  $A$  as in Eqn. 13:

$$f(\tau_X(N)) = A N^2 \frac{2S(S+1)}{3\langle \vec{S}_0 \cdot \vec{S}_1 \rangle^2} \times \left[ \left(5 - \frac{\pi^2}{N^{2/3}}\right) \frac{|t|}{J'} - \frac{S}{2} \right]^2. \quad (\text{C5})$$

$f(t)$  could be expanded about  $t = \tau_S$  to obtain an explicit expression for  $\tau_X(N)$ . However, it is clear that large band states rarely cross the polaron level.  $f(t)$  on

the LHS is bounded from above by 1 and the RHS is proportional to  $N^2$ , and so only small band states satisfy Eqn. C5. Since  $\tau_N$  grows with  $N$ , the size of the largest crossing band state follows from Eqn. C4 in the limit  $\tau_X(N) \rightarrow \infty$ . In this limit  $f(t) = 1$  so that the largest crossing band state needs  $N \sim \langle \vec{S}_0 \cdot \vec{S}_1 \rangle^2 \ll 1$ . This result shows that large band states do not cross the polaron level according to Gaussian statistics. The physical reason is that the contribution to the  $s$ - $d$  energy of a single pair of local moments is weighted by the electron density. For large states this density is low, so that alignment of a single pair of local moments does not lower the energy significantly. Thus, a crossing requires all the local moments to fluctuate into nearly perfect alignment. Of course, large clusters of ferromagnetically aligned local moments do exist, and do cross the polaron level, but they lie in the far tail of the band and are far more rare than a Gaussian approximation to the density of states would predict. These fluctuations are thus negligible. We have therefore shown that our expressions for  $\tau_X$  in Eqn (14) and (15) give the correct hopping rate for the small FMP.

- 
- <sup>1</sup> P. Majumdar and P. B. Littlewood. *Phys. Rev. Lett.*, 81:1314, 1998.
  - <sup>2</sup> P. Majumdar and P. B. Littlewood. *Nature*, 395:479, 1998.
  - <sup>3</sup> M. J. Calderón and P. B. Littlewood. *preprint condmat/9911109*, 1999.
  - <sup>4</sup> B. Martinez, R. Senis, J. Fontcuberta, and X. Obradors. Carrier density dependence of magnetoresistance in  $\text{Ti}_2\text{Mn}_{2-x}\text{Ru}_x\text{O}_7$  pyrochlores. *Phys. Rev. Lett.*, 83(10):2022, 1999.
  - <sup>5</sup> Y. Shimikawa, Y. Kubo, and T. Manako. *Nature*, 379:53, 1996.
  - <sup>6</sup> A. P. Ramirez and M. A. Subramanian. *Science*, 277:546, 1997.
  - <sup>7</sup> M. Y. Kagan, D. I. Khomskii, and M. V. Mostovoy. *Physica B*, 243:1209, 2000.
  - <sup>8</sup> A. Moreo, S. Yunoki, and E. Dagotto. *Science*, 283:2034, 1999.
  - <sup>9</sup> G. Allodi, R. De Renzi, and G. Guidi. <sup>139</sup>La NMR in lanthanum manganites: Indication of the presence of magnetic polarons from spectra and nuclear relaxations. *Phys. Rev B*, 57(2):1024, 1998.
  - <sup>10</sup> C. S. Snow et al. *preprint condmat/0011527 v3*, 2000.
  - <sup>11</sup> P. Nyhus, S. Yoon, M. Kaufmann, S. L. Cooper, Z. Fisk, and J. Sarrao. Spectroscopic study of bound magnetic polaron formation and the metal-semiconductor transition in  $\text{EuB}_6$ . *Phys. Rev. B*, 56(5):2717, 1997.
  - <sup>12</sup> E.D. Isaacs, D. Heimann, M. J. Graf, B. Goldberg, R. Kershaw, D. Ridgley, K. Dwight, A. Wold, J. Furdyna, and J. S. Brooks. Bound magnetic polarons below  $T = 1\text{K}$ . *Phys. Rev. B*, 37(12):7108, 1988.
  - <sup>13</sup> S. von Molnar and S. Methfessel. *J. Appl. Phys.*, 38:959, 1967.
  - <sup>14</sup> P. A. Wolff. In J. K. Fudyna and J. Kossut, editors, *Semiconductors and Semimetals*, volume 25, chapter 10. Academic Press, New York, 1988.
  - <sup>15</sup> T. Kasuya, A. Yanase, and T. Takeda. *Sol. St. Comm.*, 8:1543, 1970.
  - <sup>16</sup> E. L. Nagaev. *Sov. Phys. Solid State*, 13:961, 1971.
  - <sup>17</sup> C. Benoit à la Guillaume. *Phys. Stat. Sol. (b)*, 175:369, 1993.
  - <sup>18</sup> E. M. Kogan and M. I. Auslender. *Phys. Stat. Sol. (b)*, 147:613, 1988.
  - <sup>19</sup> S. Chandrasekhar. *Rev. Mod. Phys.*, 15:1, 1943.
  - <sup>20</sup> S. Chandrasekhar. *Rev. Mod. Phys.*, 21:383, 1949.
  - <sup>21</sup> S. W. Lovesey. *Condensed Matter Physics: Dynamic Correlations*. Benjamin Cummings, 2<sup>nd</sup> edition, 1986.
  - <sup>22</sup> J. Hubbard. *J. Phys. C: Solid St. Phys.*, 4:53, 1971.
  - <sup>23</sup> M. Blume and J. Hubbard. Spin-correlation functions at high temperatures. *Phys. Rev. B*, 1(9):3815, 1970.
  - <sup>24</sup> C. Zener. *Proc. Roy. Soc.*, A137:696, 1932.
  - <sup>25</sup> L. D. Landau. *Phys. Z. USSR.*, 1:426, 1932.
  - <sup>26</sup> S-W. Cheong, H. Y. Hwang, et al. *Sol. St. Comm.*, 98:163, 1996.
  - <sup>27</sup> A. Alonso, J. L. Martínez, M. J. Martínez-Lope, and M. T. Casais. *Phys. Rev. Lett.*, 82:89–192, 1999.
  - <sup>28</sup> J. C. Cooley, M. C. Aronson, J. L. Sarrao, and Z. Fisk. High pressure and ferromagnetic order in  $\text{EuB}_6$ . *Phys. Rev. B*, 56(22):14541, 1997.
  - <sup>29</sup> S. Süllow, I. Prasad, et al. Structure and magnetic order of  $\text{EuB}_6$ . *Phys. Rev. B*, 57:5860, 1998.